

# Spatiotemporal distribution and short-term trends of particulate matter concentration over China, 2006–2010

Ling Yao · Ning Lu

Received: 12 August 2013 / Accepted: 1 May 2014 / Published online: 15 May 2014  
© Springer-Verlag Berlin Heidelberg 2014

**Abstract** Air quality problems caused by atmospheric particulate have drawn broad public concern in the global scope. In the paper, the spatiotemporal distributions of fine particle (PM<sub>2.5</sub>) and inhalable particle (PM<sub>10</sub>) concentrations estimated with the artificial neural network (ANN) over China during 2006 to 2010 have been discussed. Most high PM<sub>10</sub> concentration appears in Xinjiang, Qinghai, Gansu, Ningxia, Hubei, and parts of Inner Mongolia. The distribution of PM<sub>2.5</sub> concentration is consistent with China's three gradient terrains. The seasonal variations of PM<sub>2.5</sub> and PM<sub>10</sub> concentrations both indicate that they are higher in north China in spring and winter, lowest in summer. In autumn, most provinces in south China appear high value. In particular, high PM<sub>2.5</sub> concentration appears in the southeast coastal cities while high PM<sub>10</sub> concentration prefers the central regions in south China. On this basis, seasonal Mann–Kendall test method is utilized to analyze the short-term trends. The results also show significant changes of PM<sub>2.5</sub> and PM<sub>10</sub> concentrations of China in the past 5 years, and most provinces present the tendency of reduction (3–5  $\mu\text{g}/\text{m}^3$  for PM<sub>2.5</sub> and 10–20  $\mu\text{g}/\text{m}^3$  for PM<sub>10</sub> per year) while a fraction of provinces appear the increasing trend of 8–16  $\mu\text{g}/\text{m}^3$  (PM<sub>2.5</sub>) and 16–30  $\mu\text{g}/\text{m}^3$  (PM<sub>10</sub>). Simultaneously, PM<sub>2.5</sub> population exposure is discussed with the combination of population density-gridded data. Municipalities get much higher exposure level than other provinces. Shanghai suffers the highest population exposure to PM<sub>2.5</sub>, followed by Beijing and then Tianjin, Jiangsu province. Most provincial capitals, such as

Guangzhou, Nanjing, Chengdu, and Wuhan, face much higher exposure level than other regions of their province. Moreover, the PM<sub>2.5</sub> exposure situation is more serious in southeast than northwest regions for Beijing-Tianjin-Hebei region. Also, per capita PM<sub>2.5</sub> concentration and population-weighted PM<sub>2.5</sub> concentration are calculated. The former shows that the high-level regions distribute in Guangdong, Shanghai, and Tianjin, while the latter in Hebei, Chongqing, and Shandong provinces. Further studies may consider optimizing concentration estimation model and use it to discuss the effects of particulate matters on human health.

**Keywords** Artificial neural network (ANN) · Fine particles (PM<sub>2.5</sub>) · Inhalable particles (PM<sub>10</sub>) · Satellite remote sensing · Spatiotemporal distribution

## Introduction

Along with the acceleration of urbanization process, air quality has become an important protection factor which influences urban sustainable development and ecological city construction. Particulate matter is one of the major pollutants that affect air quality in urban and even rural areas of the world (Gupta et al. 2006). The particles with aerodynamic diameters less than 2.5  $\mu\text{m}$  are defined as fine particles (PM<sub>2.5</sub>) (Liu et al. 2005, 2009), while less than 10  $\mu\text{m}$  are called inhalable particles (PM<sub>10</sub>). The density of PM<sub>2.5</sub> ground observation network in China is relatively low, and the distribution of observation stations is uneven, so it's difficult to reflect the spatial distribution characteristics of PM<sub>2.5</sub> according to the ground monitoring data alone.

Remote-sensing techniques, which provide consistent measurements at broad-scale and frequent time intervals, have been increasingly adopted to assess surface level of particulate matter concentration at high spatial and temporal resolutions

Responsible editor: Gerhard Lammel

L. Yao · N. Lu (✉)  
State Key Laboratory of Resources and Environmental Information System, Institute of Geographic Sciences and Natural Resources Research, Chinese Academy of Sciences, No.11A, Datun Road, Chaoyang, Beijing 100101, China  
e-mail: ning.robin@gmail.com

(Gupta and Christopher 2009a). Martin (2008) has reviewed the state-of-arts satellite remote-sensing sensors for air quality monitoring, and it has been revealed that aerosol remote sensing at visible wavelengths exhibits high sensitivity to boundary layer concentrations. A rigorous review of the sensors' characteristics led to the hypothesis that moderate resolution imaging spectroradiometer (MODIS) instrument is most likely to achieve the best results and has been utilized to retrieve aerosol optical thickness (AOT) (Kaufman et al. 1997; Tanré et al. 1997). Wang and Christopher (2003) have demonstrated that satellite-derived AOT is a good surrogate for monitoring particulate matter air quality over the earth.

Wang and Martin (2007) have estimated near ground PM<sub>2.5</sub> concentration in Beijing area with MODIS 1 km data based on the vertical and humidity correction of AOT inversion; the correlation with observed values is relatively high ( $R^2=0.47$ ). Liu et al. (2005) have used aerosol vertical profiles simulated by atmospheric chemistry model to the vertical correction of satellite remote sensing AOT and extracted the extinction contribution of surface layer aerosol which can reflect better changes of near ground particles ( $R^2=0.46$ ). Van Donkelaar et al. (2006) have demonstrated that the main influence factor between AOT and PM<sub>2.5</sub> is the relative vertical profiles of aerosol extinction coefficient. Then, Donkelaar et al. (2010) have given a map of the average PM<sub>2.5</sub> concentration from 2001 to 2006; in this map, even the relatively low PM<sub>2.5</sub> concentration in east China is about 60–90  $\mu\text{g}/\text{m}^3$ , while the high value is more than 100  $\mu\text{g}/\text{m}^3$ . What's more, the research also points out that the value is still 25 % lower than the real situation in some areas.

The works have considered the influence of various environmental, meteorological factors on AOT–PM<sub>2.5</sub> relationship, using multivariate statistical regression model to describe the relationship between near ground particulate concentration and multiple factors including AOT. However, the regression equation is only applicable to the estimation of average conditions, a situation that underestimates high concentration or overestimates low concentration would arise (Gupta and Christopher 2009a). Previous research has shown that the artificial neural network (ANN) can achieve a better inversion of particulate concentration by introducing the meteorological factors in the process of constructing appropriate satellite AOT–PM relationship (Gupta and Christopher 2009b).

In this paper, ANN (Matthew 1990) is developed with satellite, ground, and meteorological data sources to assess the concentration of particulate matter. The spatiotemporal distribution of PM<sub>2.5</sub> and PM<sub>10</sub> concentration and also the short-term trends over China in the period of 2006 and 2010 have been analyzed. Furthermore, population exposure to PM<sub>2.5</sub> of China in 2010 has been discussed and the per capita PM<sub>2.5</sub> concentration and the population-weighted PM<sub>2.5</sub> concentration have been calculated.

The rest of this paper is organized as follows. In Section “Data and methodology,” we give a brief description on the data sources and the mechanisms and schedules of proposed methods for particulate matter concentration estimation and short-term trends analysis. The spatiotemporal distribution and short-term trends of particulate matter concentration in the past 5 years over China are clarified and discussed in Section “Results and discussion.” Finally, a conclusion is drawn in Section “Conclusions.”

## Data and methodology

### Study area

For covering particulate matter problem in China, our spatial domain includes mainland China (excludes Hainan, Hongkong, Macao, and Taiwan). To be sure, Hainan province, Hongkong, Macao, and Taiwan are not included in the study area because of the influence of cloud and aerosol type. Macao is also left out of the study area due to the contradiction between its small area and spatial resolution (10 km) of the estimated concentration.

### Data sources

Four data sources are used in the study; the details of data sources and their uncertainties are as follows.

1. MODIS atmosphere aerosol product (MOD04\_L2). The MOD04\_L2 is daily level-2 data, derived from National Aeronautics and Space Administration (NASA) Terra platform. It has been produced at the spatial resolution of a  $10 \times 10$  km (at nadir) pixel array. The MOD04\_L2 product is suitable for granules where the minimum solar zenith angle is less than or equal to  $72^\circ$ . Levy and Remer (2007) demonstrated that MODIS AOD product has 10–20 % uncertainty compared with surface station observation.
2. ERA-Interim, which is the latest global atmospheric reanalysis produced by European Centre for Medium-Range Weather Forecasts (ECMWF) (Dee et al. 2011). It now extends back to 1979, and the analysis continues to be extended forward in near-real-time. More detailed description of the ERA-Interim product archive can be found in the paper of Berrisford et al. (2009). Simmons et al. (2010) have found that ERA-Interim data agrees well with Climatic Research Unit and Hadley Centre analyses of monthly station temperature data (CRUTEM3), and the correlations between the CRUTEM3 and ERA-Interim data in North America and Asia exceed 99 %.
3. Ground-observed particulate matter concentration data. Due to less monitoring data of China, some American site

monitoring data derived from the US Environmental Protection Agency (EPA) is used in this paper. Considering the fact that particulate matter concentration in China is much higher than USA, ground-observed particulate matter concentration data of China is introduced to achieve a more plausible estimation model.

The EPA and its partners in the USA set up the air quality monitoring network to collect ground-level particulate matter concentration in air pollution monitoring. Total suspended particulate (TSP), PM10, and PM2.5 concentrations were obtained according to EPA-defined methodology.

We consider monitoring data as the gold standard here, while acknowledging that the ground measurements are not error-free (instrument error variance of approximately 1.5 based on colocated monitors, relative to a trimmed variance of the measurements of 60) (Christopher et al. 2008). To assess the relationship between PM2.5 and AOD, we matched monitoring data to the nearest AOD pixel, omitting a small number of monitors for which the nearest pixel centroid is closer to another monitor.

The AOD–PM relationship varies by region and aerosol characteristics, but network generalization can be improved by ensuring that the training data are extensive and comprehensive. An extensive training set would include all geographic regions of the Earth, all seasons, night and day cases, and so forth (Blackwell and Chen 2009). In this paper, the utilization of the US monitoring data along with the Chinese monitoring data is to assure the training dataset contains extensive sampling (that is, high, medium, and low monitoring values).

4. Gridded population dataset, which is derived from the Center for International Earth Science Information Network (CIESIN), contains the distribution of human population. It is a gridded data product that renders global population data at the scale and extent required to demonstrate the spatial relationship of human population and the environment across the globe.

### Particulate matter concentration estimation

The ANN algorithm, which is designed for modeling complex relationships between inputs and outputs or to find patterns in data, has been proved to solve this problem (Gupta and Christopher 2009a, b; Yao et al. 2012a).

An ANN is typically defined by three types of layers of units: input, hidden, and output. Each layer can contain multiple neurons. A layer of input units is connected to a layer of hidden units, which is connected to a layer of output units. With the use of input and output sample sets, network structure builds up network-mapping relationship on a given input and output through its training, learning, and adjustment of

neural network weights and thresholds. Trained network will be able to grasp the essential characteristics, not only in the input sample dataset but also in the given appropriate output dataset, that is, with the generalization. It is trained using the traditional error back-propagation (BP) algorithm. BP neural network is a forward multilayer network, which was first developed by Rumelhart et al. (1986). Besides, in order to minimize the error sum of squares, the Levenberg–Marquardt (LM) algorithm (Levenberg 1944) was utilized to improve BP network training. LM algorithm is an effective method of nonlinear least squares problem. It is superior to conventional BP algorithm with fast convergence and high approximation accuracy.

In this study, there are eight parameters in the input units of the constructed neural network, including latitude, longitude, single scattering albedo (SSA), aerosol optical thickness (AOT), wind speed, relative humidity, skin temperature (SKT), and planetary boundary layer height. Where, the AOT and SSA are retrieved from MODIS instruments, and the last four parameters are derived from ERA-Interim. There are 16 hidden layers in the constructed neural network model. The performance of the network is evaluated by calculating absolute percentage errors (APE) (Gupta and Christopher 2009a),

$$APE = \frac{100 \times (|Y_{est} - Y_{obs}|)}{(|Y_{obs}|)} \tag{1}$$

where,  $Y_{est}$  is the estimated particulate matter concentration using trained network, and  $Y_{obs}$  is the observed particulate matter concentration in validation data set.

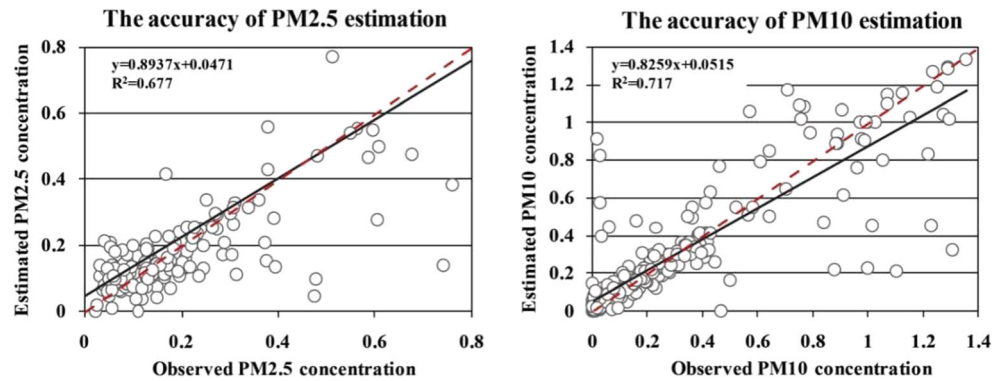
To construct an ANN model for the particulate matter concentration estimation, about 1,078 samples distributed over USA and China have been used. The samples are randomly assigned to be three subsets. That is, 40 % samples are selected for training, 20 % for testing, and remaining 40 % are used for model validation.

Figure 1a, b shows the correlation between estimated results and ground monitoring values on the concentration of PM10 and PM2.5, respectively. The correlation coefficient (Heij et al. 2004) and APE are also calculated between the matched pairs of the estimated result and ground monitoring value to evaluate the estimation accuracy. The correlation coefficients of PM2.5 and PM10 are, respectively, 0.82 and 0.85, while the APEs are, respectively, about 25 and 29 %, respectively. The results demonstrate the feasibility of the proposed ANN model on estimating the concentration of particulate matter, and the constructed model will be utilized in China.

### Short-term trend analysis

We first used least-square method to linearly fit the monthly average atmospheric particulate matters (PM10 and PM2.5).

**Fig. 1** Accuracy of particulate estimation concentration



The results can reflect the interannual short-term trends of China. However, singular value may affect the results due to the shortage of the time series. Thus, a nonparameter Mann–Kendall test (Mann 1945) method was utilized to analyze the trends of time series and decrease the effect of possible singular values. Mann–Kendall test is used to assess the significance of the trend. It can be stated most generally as a test for whether estimated results tend to increase or decrease with ground monitoring values (monotonic change). However, the monthly observation sequence is typically seasonal distribution. Hirsch et al. (1982) improved the traditional Mann–Kendall method and developed the seasonal-based method (seasonal Mann–Kendall) to solve this problem. This method could be effective in preventing the disturbance that the abnormal value may have on judging the time series trend (Partal and Kahya 2006). In the meanwhile, it does not require the sample to be normally distributed and will not be affected by certain lack of value in the time series.

In this research, the trend is calculated with the monthly average value of the mentioned 5 years, meanwhile, we have considered the seasonal distribution of PM, so the seasonal Mann–Kendall trend test is used in the research. That is, 60 effective values are involved in the seasonal Mann–Kendall trend test. We have also performed significance test in the research, and the blank area in the figures means the short-term trend in these regions cannot pass through the significance test. The trend is calculated with monthly average value but indicates the yearly short-term changing characteristic. The details about seasonal Mann–Kendall test method can be found in Hirsch et al. (1982) and Yao et al. (2012b).

#### Population exposure assessment

Based on the yearly average PM<sub>2.5</sub> concentration, we calculate an indicator (P-E) for long-term population exposure assessment. It's calculated with Eq. 2 based on grid computing. Then, a provincial statistics is

performed to access the population exposure in the provincial scale.

$$P-E = (PM_i - \text{threshold value}) \times P_i \quad (2)$$

where,  $PM_i$  is defined as the  $i$ th pixel value of PM<sub>2.5</sub> concentration,  $P_i$  is the  $i$ th pixel value of population density. According to the WHO recommended value, the threshold value in Eq. 2 is  $10 \mu\text{g}/\text{m}^3$ .

In the meanwhile, we also calculate per capita PM<sub>2.5</sub> concentration (P-C) with population-weighted PM<sub>2.5</sub> concentration (P-W). Maybe, they are not about population exposure but useful to population health assessment while used in conjunction with incidence data of disease. P-C indicates the average experience of PM<sub>2.5</sub> in a certain province, while P-W is emphasis on the actual experience to resident, that is, the weightiness of PM<sub>2.5</sub> concentration in population density area is larger than suburb or population sparse area. They are, respectively, calculated with Eqs. 3 and 4.

$$P-C = \frac{\sum_{i=1}^n PM_i}{n} \quad (3)$$

$$P-W = \frac{\sum_{i=1}^n PM_i \times P_i}{\sum_{i=1}^n P_i} \quad (4)$$

where,  $PM_i$  is defined as the  $i$ th pixel value of PM<sub>2.5</sub> concentration,  $P_i$  is the  $i$ th pixel value of population density, and  $n$  is the total pixel number.

## Results and discussion

#### Parameter effects and sensitivity analysis

Why not present all available inputs and let the neural network determine which are relevant? This approach is reasonable if there are no restrictions on the training set size or the time required for training. This is usually not the case, and the efficiency of the training process can be substantially



increased if excessively noisy, unimportant, or redundant inputs are removed (Blackwell and Chen 2009).

In this paper, we used stepwise regression to ascertain the input training parameters, the step-by-step iterative construction of a regression model that involves automatic selection of independent variables. The main approach used in this research is backward elimination, which involves starting with all candidate variables, testing the deletion of each variable using a chosen model comparison criterion, deleting the variable (if any) that improves the model the most by being deleted, and repeating this process until no further improvement is possible (Chatfield 1995).

As for the number of hidden nodes, it has been proven that neural networks with a single-hidden layer are universal approximators capable of representing any real-valued continuous function to arbitrary precision over a finite domain if enough hidden nodes are used. However, networks with

multiple hidden layers can sometimes perform better than single-hidden-layer networks, with fewer total nodes (Blackwell and Chen 2009).

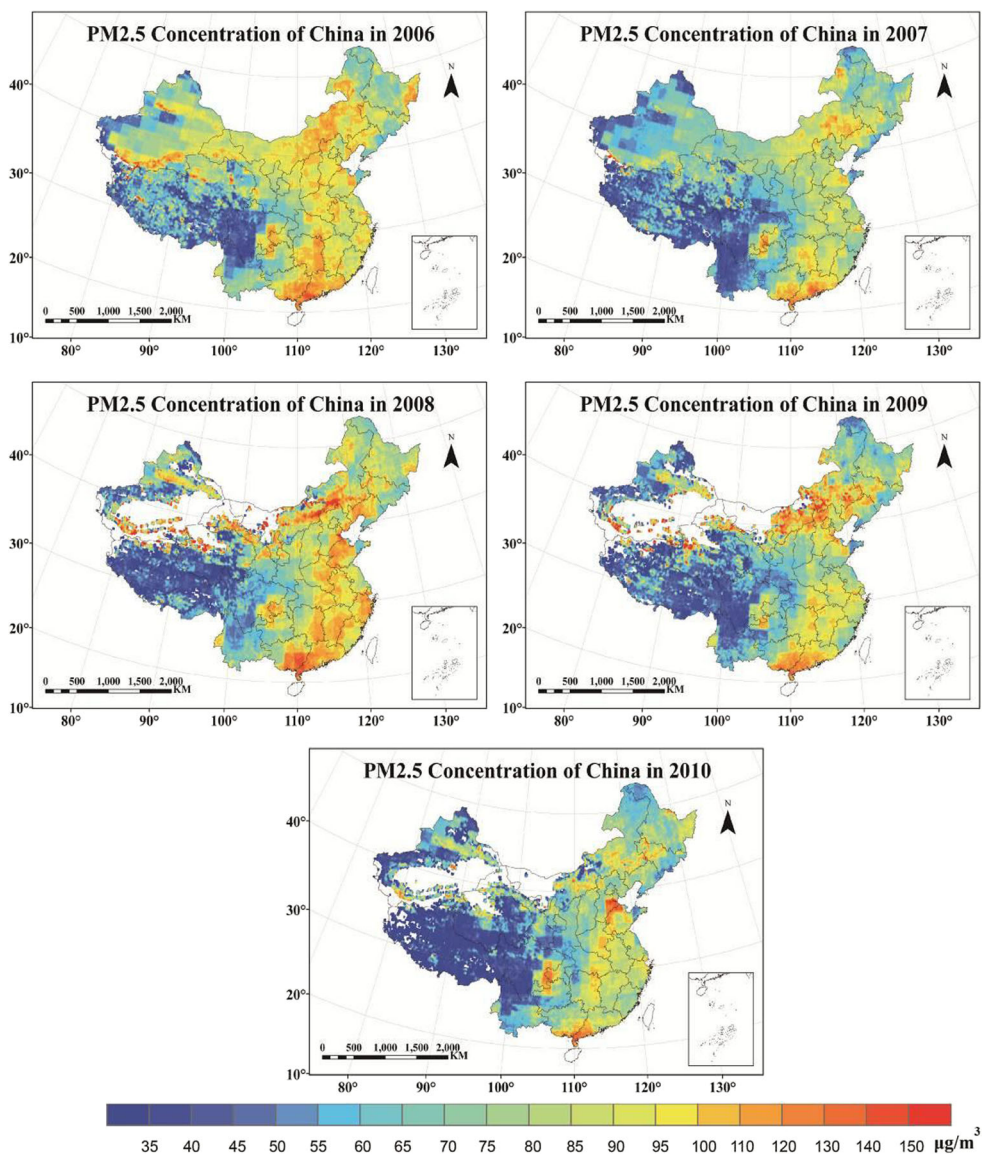
The experiment shows that over 16 hidden nodes and 9,000 runs with random sampling provided sufficient data samples for extracting the principal information of the used training data, because the satellite retrieval accuracy of PM concentration almost remained the same as the number of hidden nodes and runs increased subsequently.

Spatiotemporal distribution of particulate matter

*PM2.5 spatiotemporal distribution*

Figure 2 shows annual average of PM2.5 concentration of China during 2006 to 2010.

**Fig. 2** Annual average of PM2.5 concentration of China in the past 5 years



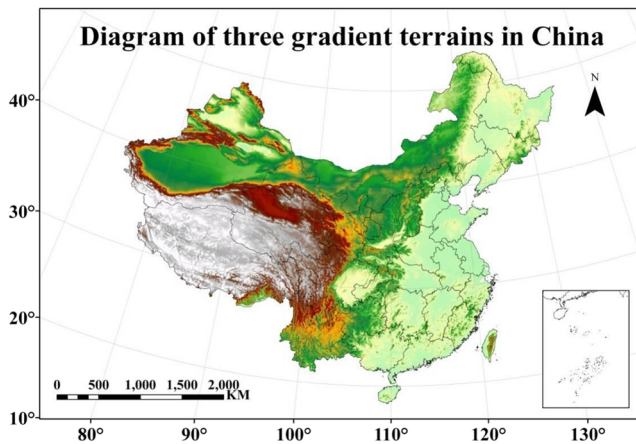


**Fig. 3** Diagram of three gradient terrains in China

Figure 3 shows the diagram of China's three gradient terrains. The "three gradient terrains" portrays an outline of terrain changes like ladders along west–east direction. The first and second gradient terrains are divided by the profile along Kunlun, Qilian, and Hengduan mountains. The second and third gradient terrains are divided by the profile along Great Khingan, Taihang, Wushan, and Xuefeng mountains. From Figs. 2 and 3, we found that the spatial distribution of annual average PM<sub>2.5</sub> concentration coincides with China's three gradient terrains.

Figure 4 shows the seasonal average of PM<sub>2.5</sub> concentration of China in 2010. Seasonal meteorological division method is used, i.e., from March to May is spring (lunar calendar),

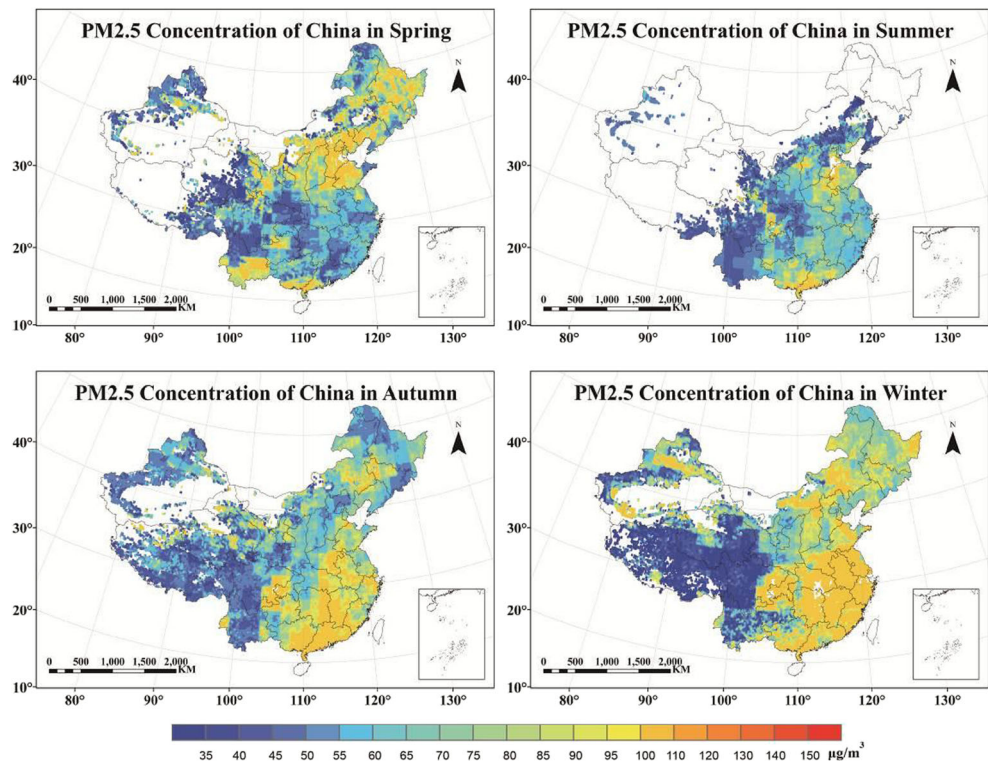
June to August is summer, September to November is autumn, and December to February next year is winter.

The results show obvious seasonal variation in China. The seasonal PM<sub>2.5</sub> concentration presents that the north is higher in the spring and winter, lowest in summer. In autumn, the PM<sub>2.5</sub> concentration of most provinces in southeast China appears high value. This may be associated with the dust weather in spring; heating system in winter, which increases the concentration of PM<sub>2.5</sub>, while the sufficient precipitation will decrease the concentration in summer. In autumn, the high value of PM<sub>2.5</sub> in southern China may be associated with straw burning after crop harvest.

#### *PM<sub>10</sub> spatiotemporal distribution*

Figure 5 shows annual average of PM<sub>10</sub> concentration of China during 2006 to 2010. During 2006 to 2008, PM<sub>10</sub> concentration of China, especially in Xinjiang, southeast coastal areas, and Guangdong province, show a clear downward trend. In 2009, the concentration of Hunan, Hubei, and adjacent provinces increased, and decreased again in 2010. There are several obvious high value regions of China in the past 5 years, such as, most of Xinjiang, Qinghai, Gansu, Ningxia, Hubei, and parts of Inner Mongolia. Some east coast provinces, e.g., Jiangsu and Anhui, are located in the median zone. The results are consistent with the 343 monitoring and statistical data released by Ministry of Environmental

**Fig. 4** Seasonal average of PM<sub>2.5</sub> concentration of China in 2010



Protection of China. Beijing is not in the high value area throughout the country and lower than its neighborhoods.

Figure 6 shows the seasonal average of PM10 concentration of China in 2010. The seasonal PM10 concentration is a bit like PM2.5 concentration; nevertheless, there are apparent differences about the high value region in autumn between them. PM2.5 high value area appears in the southeast coast cities while PM10 prefers the central regions in the southern China.

*Analysis on the spatial difference of P2.5 and PM10*

As can be seen in Figs. 2 and 5, there exists an obvious spatial difference between PM2.5 and PM10. As stated in the previous section, most high PM10 concentrate in Xinjiang, Qinghai, Gansu, Ningxia, Hubei, and parts of Inner Mongolia. Yet, the

distribution of PM2.5 concentration is consistent with China’s three gradient terrains. We could use Angstrom exponent and explain what is happening.

Figure 7 shows the distribution of Angstrom exponent in China in 2010. Angstrom exponent is the exponent in the formula that is usually used to describe the dependency of the aerosol optical thickness, or aerosol extinction coefficient on wavelength. Angstrom exponent is a useful quantity to assess the particle size of atmospheric aerosols or clouds and the wavelength dependence of the aerosol/cloud optical properties. Kaufman et al. (1997) have demonstrated the Angstrom exponent less than 0.7 for large dust particles, and the value greater than 1.8 for fine particulate matter, or smoke particles.

Angstrom exponent is inversely related to the average size of the particles in the aerosol: the smaller the particles, the larger the exponent. That is, for a given pixel in Fig. 7, the

**Fig. 5** Annual average of PM10 concentration of China in the past 5 years

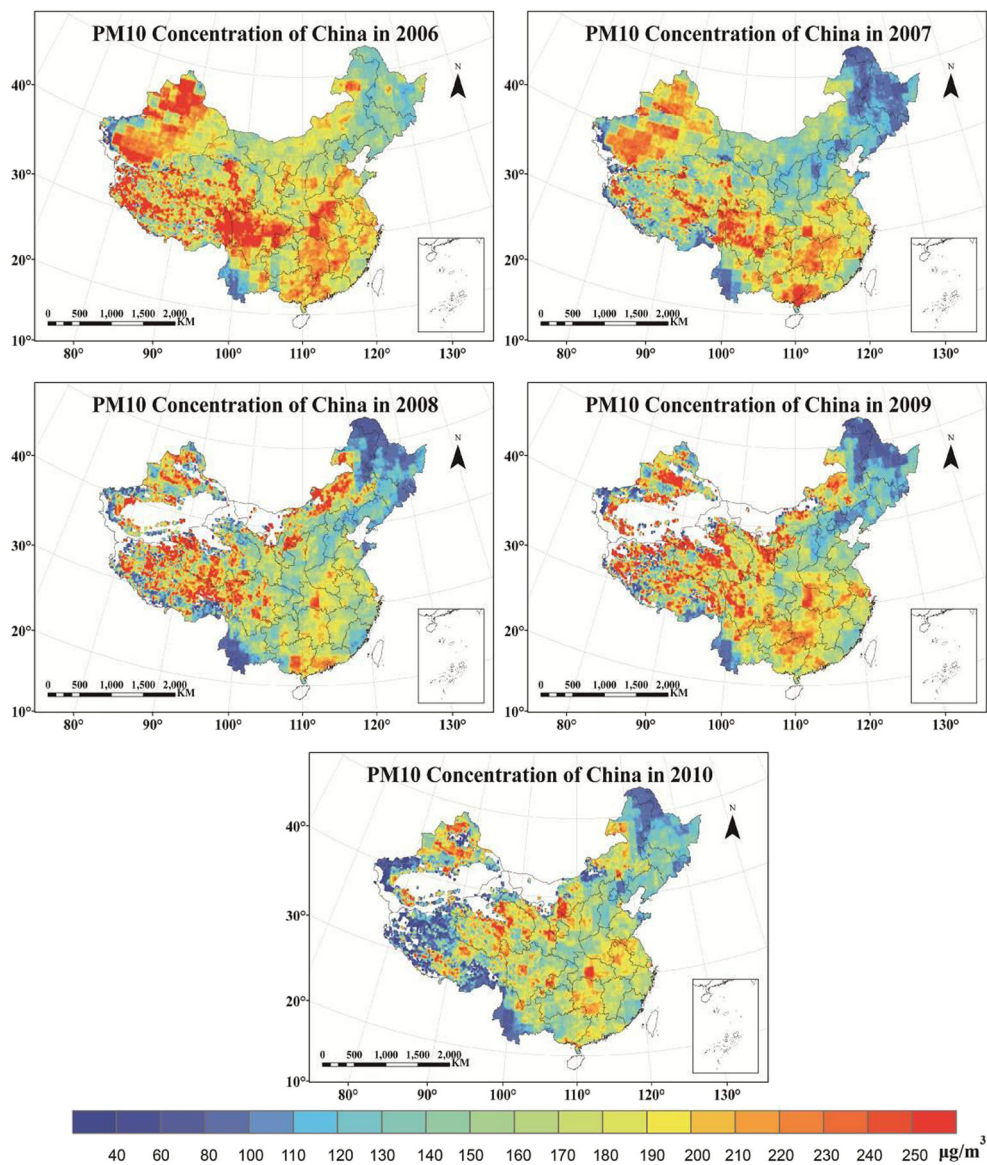
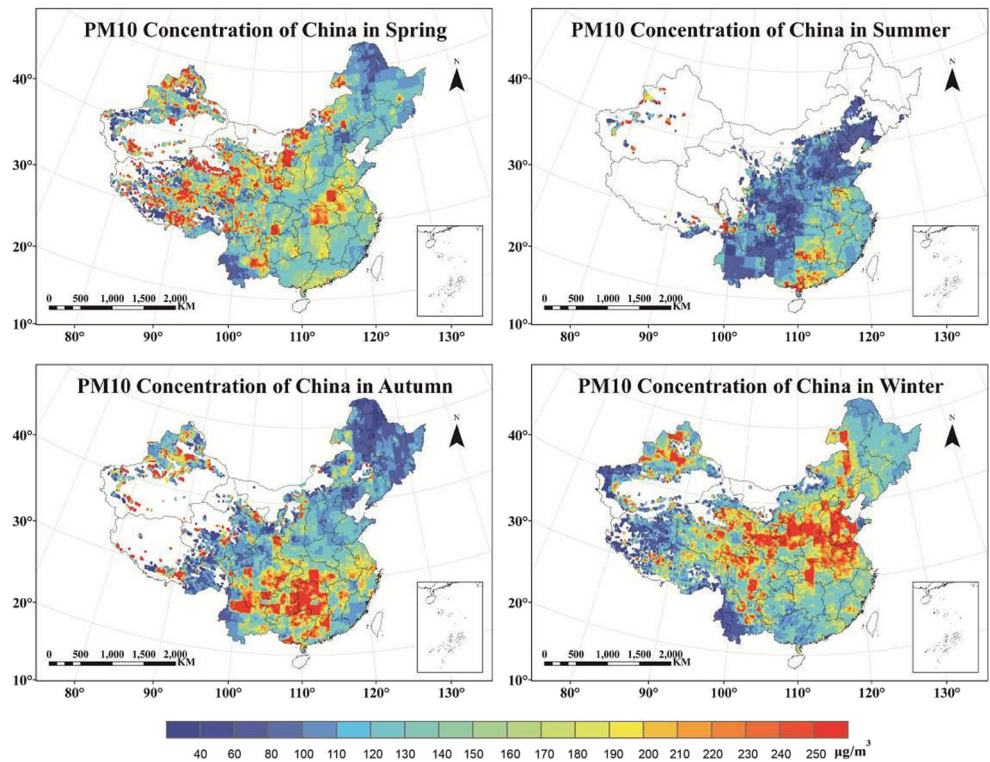




**Fig. 6** Seasonal average of PM10 concentration of China in 2010

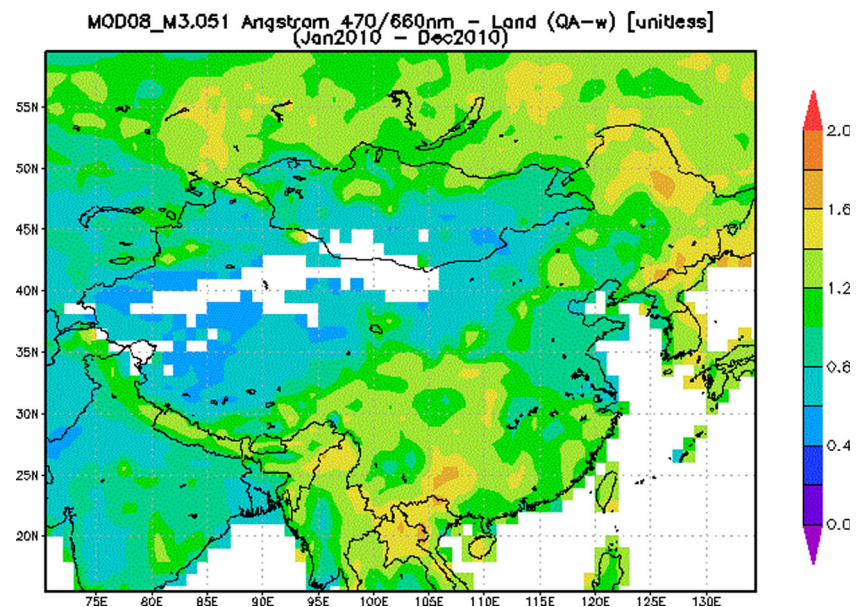


larger the Angstrom exponent value, the greater the proportion of PM<sub>2.5</sub>; the smaller the Angstrom exponent value, the greater the proportion of PM<sub>10</sub>. For example, we can see obvious high value of Angstrom exponent in Heilongjiang province in Fig. 7; the corresponding region demonstrates high PM<sub>2.5</sub> concentration (Fig. 2) and low PM<sub>10</sub> concentration (Fig. 5). It can explain the spatial difference of PM<sub>2.5</sub> and PM<sub>10</sub> concentrations in some extent.

Short-term trends of particulate matter

PM concentration changing trends consist of long-term trend and short-term trend. That is, PM concentration changing trends in China may point to a long-term increasing trend, with some short-term variability, which need to be checked in the future research. The short-term trends are not representative of the long-term changes in PM, but important when

**Fig. 7** Distribution of Angstrom exponent in China (2010). Data is from Terra MODIS





testing time series models (Foster and Rahmstorf 2011; Thompson et al. 2009).

Short-term PM variability means that individual years can have higher PM concentrations than the previous year, while the underlying decreasing trend continues. Short-term variations in PM may be due to the government behavior. For example, Beijing adopted many prevention and control measures to improve air quality for the 29th Olympic Games in 2008 (Zhang et al. 2010).

We adopted seasonal Mann–Kendall test to detect the short-term trends of PM concentrations. It is a rank-based procedure, which is robust to the influence of extremes and good for use with skewed variables (Partal and Kahya 2006). Figure 8 shows the significant changes of PM2.5 and PM10 of China in the past 5 years. The blank area in the figures means the change trends are not significant in these regions.

For PM10, most provinces present the tendency of reduction. The declination of concentration is about 10–20  $\mu\text{g}/\text{m}^3$ . Few of provinces show increase, such as Gansu, Shaanxi, Sichuan, Guizhou, and Guangdong. Besides, in Henan, Anhui, Jiangsu, and Hunan, the concentration is also increasing, and the corresponding level is about 16–30  $\mu\text{g}/\text{m}^3$ .

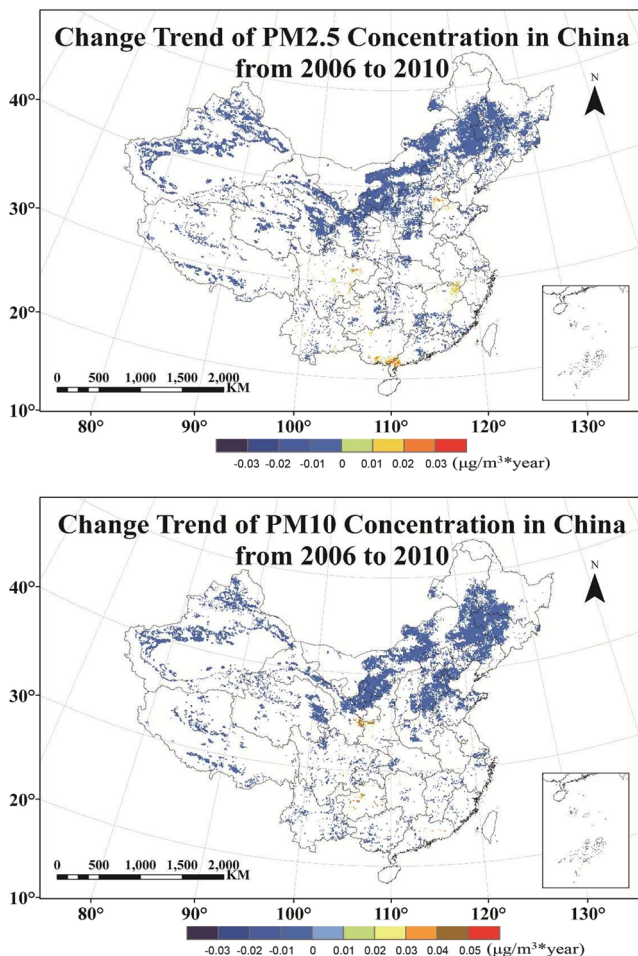


Fig. 8 Change trends of PM2.5 and PM10 in China from 2006 to 2010

PM2.5 shows the same change trend as PM10; most provinces present the tendency of reduction. The declination of concentration is about 3–5  $\mu\text{g}/\text{m}^3$ . Few of provinces show increase, such as Hebei, Shandong, Anhui, Jiangxi, Guangdong, Guangxi, Sichuan, and Guizhou. The corresponding level is about 8–16  $\mu\text{g}/\text{m}^3$ .

Population exposure to PM2.5

Chinese long-term population exposure to PM2.5 in 2010 is shown in Fig. 9. The spatial distribution of the results is illustrated in both grid level and provincial level. It can be seen from the provincial statistics figure that municipalities get much higher exposure level than other provinces. Shanghai suffers the highest population exposure to PM2.5, followed by Beijing and then Tianjin, Jiangsu province. On the other hand, the grid-scale map demonstrates the spatial distribution of population exposure to PM2.5. Obviously, there is a totally different population exposure level even in a certain province. Most provincial capitals, such as Guangzhou, Nanjing, Chengdu, and Wuhan, face much higher exposure level than other regions of their province.

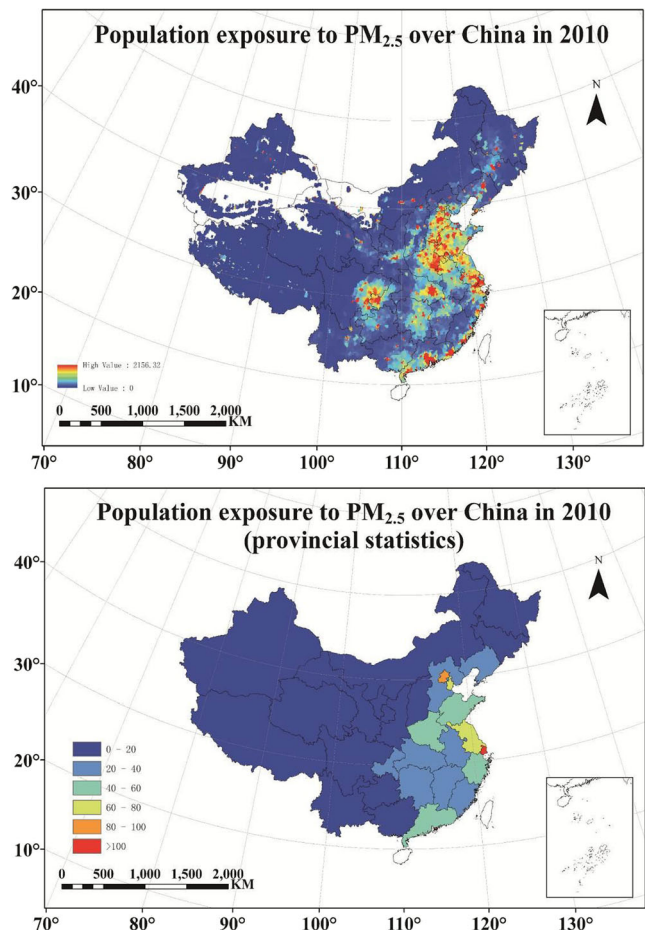


Fig. 9 PM2.5 population exposure level of China in 2010

**Table 1** Provincial P-C and P-W PM<sub>2.5</sub> concentration statistics of China in 2010 ( $\mu\text{g}/\text{m}^3 \cdot \text{person}$ )

Province	Per capita	P-W	Province	Per capita	P-W
Beijing	78.58	13.55	Henan	86.6	15.25
Tianjin	98.18	13.57	Hubei	79.2	14.96
Hebei	86.96	15.9	Hunan	82.8	14.98
Shanxi	76.7	13.3	Guangdong	97	15.5
Inner Mongolia	74.78	14.69	Guangxi	84.4	15.1
Liaoning	76.1	13.06	Chongqing	83.6	16.39
Jilin	78.46	14.82	Sichuan	52.89	12.48
Heilongjiang	74	13.6	Guizhou	71.7	12.47
Shanghai	104	15.48	Yunnan	55.99	10
Jiangsu	86.88	14.99	Xizang	32.44	6
Zhejiang	88.88	15	Shannxi	63.6	11.15
Anhui	88	15.2	Gansu	63.69	10
Fujian	79.57	12.99	Qinghai	45.95	8.8
Jiangxi	85.4	14.88	Ningxia	74.4	12.9
Shandong	92.6	15.61	Xinjiang	56.49	9

Moreover, the PM<sub>2.5</sub> exposure situation is more serious in southeast than northwest regions for Beijing-Tianjin-Hebei region.

The calculated results of per capita PM<sub>2.5</sub> concentration and population-weighted PM<sub>2.5</sub> concentration are summarized in Table 1. Provinces with highest per capita PM<sub>2.5</sub> concentration are Guangdong, Shanghai, and Tianjin. The following higher places are Shandong, Anhui, and Zhejiang provinces. The high-level areas of population-weighted PM<sub>2.5</sub> concentration are Hebei, Chongqing, and Shandong provinces, and followed by Henan, Anhui, Zhejiang, Guangdong, and Guangxi provinces. That is, the per capita PM<sub>2.5</sub> concentration in Guangdong, Shanghai, and Tianjin is totally high, but population in the potential high pollution area is sparse.

Although the per capita PM<sub>2.5</sub> concentration in Hebei and Chongqing is lower than the high-level area, the population in the potential high pollution area is denser. Shandong province is a special case; it not only locates in the high-level concentration area, but also the population in the potential high pollution area is dense.

## Conclusions

The main purpose of this paper is to describe the spatiotemporal distribution and short-term trends of fine particle (PM<sub>2.5</sub>) and inhalable particle (PM<sub>10</sub>) concentration over the China in the period of 2006–2010. Several data sets are used, e.g., MODIS atmosphere aerosol product, ERA-Interim, ground-based particulate matter observations, and gridded

population dataset. The artificial neural network (ANN) was utilized to estimate the concentration of particulate matter, and seasonal Mann–Kendall test method was utilized to analyze the short-term trends.

Most high PM<sub>10</sub> concentration appears in Xinjiang, Qinghai, Gansu, Ningxia, Hubei, and parts of Inner Mongolia. The distribution of PM<sub>2.5</sub> concentration is consistent with China's three gradient terrains. The results also show that the interannual PM<sub>10</sub> and PM<sub>2.5</sub> concentrations in the past 5 years present downward short-term trend, on the whole. The declinations of PM<sub>2.5</sub> concentration and the PM<sub>10</sub> concentration in most provinces are, respectively, about 3–5 and 10–20  $\mu\text{g}/\text{m}^3$ , while a fraction of provinces appear in the increasing trend of 8–16 and 16–30  $\mu\text{g}/\text{m}^3$ .

Municipalities get much higher exposure level than other provinces. Shanghai suffers the highest population exposure to PM<sub>2.5</sub>, followed by Beijing and then Tianjin, Jiangsu province. Most provincial capitals, such as Guangzhou, Nanjing, Chengdu, and Wuhan, face much higher exposure level than other regions of their province. Moreover, the PM<sub>2.5</sub> exposure situation is more serious in southeast than northwest regions for Beijing-Tianjin-Hebei region. The per capita PM<sub>2.5</sub> concentration shows that the high-level regions concentrated in Guangdong, Shanghai, and Tianjin while the population-weighted PM<sub>2.5</sub> concentrated in Hebei, Chongqing, and Shandong provinces in 2010.

Further improvements on the models should consider the optimization of parameters by using more robust historical data to train and select parameters. The proposed method could be used as a supplementary tool in aid of station monitoring. Moreover, it can also be used to discuss the human health effects of particulate matter while integrated with respiratory tract disease morbidity data.

**Acknowledgments** This work is supported by grants from the National Natural Science Foundation of China (Grants No. 41301380 and No. 41371016), Research on PM<sub>2.5</sub> Remote Sensing monitoring key technology and operational method in central-eastern China (Grant No.201309011), and China Postdoctoral Science Foundation (Grant No. 2013M542086).

## References

- Berrisford P, Dee DP, Fielding K, Fuentes M, Kallberg P, Kobayashi S, Uppala SM (2009) The ERA-Interim archive. In: ERA Report Series, No.1. ECMWF: Reading, UK
- Blackwell WJ, Chen FW (2009) Neural networks in atmospheric remote sensing. Artech House, US
- Chatfield C (1995) Model uncertainty, data mining and statistical inference. *J R Stat Soc A* 158(3):419–466
- Christopher JP, Liu Y, Hortensia MM, Shobha K (2008) Spatiotemporal associations between GOES aerosol optical depth retrievals and ground-level PM<sub>2.5</sub>. *Environ Sci Technol* 42:5800–5806
- Dee DP, Uppala SM, Simmons AJ, Berrisford P, Poli P, Kobayashi S et al (2011) The ERA-Interim reanalysis: configuration and performance

- of the data assimilation system. *Q J R Meteorol Soc* 137(656):553–597
- Donkelaar VA, Martin RV, Brauer M (2010) Global estimates of ambient fine particulate matter concentrations from satellite-based aerosol optical depth: development and application. *Environ Health Perspect* 118(6):847
- Foster G, Rahmstorf S (2011) Global temperature evolution 1979–2010. *Environ Res Lett* 6:044022
- Gupta P, Christopher SA (2009a) Particulate matter air quality assessment using integrated surface, satellite, and meteorological products: 2. A neural network approach. *J Geophys Res* 10(114), D20205
- Gupta P, Christopher SA (2009b) Particulate matter air quality assessment using integrated surface, satellite, and meteorological products: multiple regression approach. *J Geophys Res* 7(114), D14205. doi:10.1029/2008JD011496
- Gupta P, Christopher SA, Wang J, Gehrig R, Lee Y, Kumar N (2006) Satellite remote sensing of particulate matter and air quality assessment over global cities. *Atmos Environ* 40(30):5880–5892
- Heij C, Boer PD, Franses PH, Kloek T, Dijk HKV (2004) *Econometric methods with applications in business and economics*. Oxford University Press Inc., New York
- Hirsch RM, Slack JR, Smith RA (1982) Techniques of trend analysis for monthly water quality data. *Water Resour Res* 18(1):107–121
- Kaufman YJ, Tanr D, Remer LA, Vermote EF, Chu A, Holben BN (1997) Operational remote sensing of tropospheric aerosol over land from EOS moderate resolution imaging spectroradiometer. *J Geophys Res* 102(D14):17051–17067
- Levenberg K (1944) A method for the solution of certain non-linear problems in least squares. *Q Appl Math I- I(2):164–168*
- Levy RC, Remer LA (2007) Second-generation operational algorithm: retrieval of aerosol properties over land from inversion of moderate resolution imaging spectroradiometer spectral reflectance. *J Geophys Res*. doi:10.1029/2006JD007811
- Liu Y, Samat JA, Kilaru V, Jacob DJ, Koutrakis P (2005) Estimating ground-level PM<sub>2.5</sub> in the eastern United States using satellite remote sensing. *Environ Sci Technol* 39(9):3269–3278
- Liu Y, Paciorek CJ, Koutrakis P (2009) Estimating regional spatial and temporal variability of PM<sub>2.5</sub> concentrations using satellite data, meteorology, and land use information. *Environ Health Perspect* 117(6):886–892
- Mann HB (1945) Nonparametric tests against trend. *Econometrica* 13(3): 245–259
- Martin RV (2008) Satellite remote sensing of surface air quality. *Atmos Environ* 42(34):7823–7843
- Matthew Z (1990) *Neural network models in artificial intelligence*. Ellis Horwood Limited, Chichester
- Partal T, Kahya E (2006) Trend analysis in Turkish precipitation data. *Hydrol Process* 20(9):2011–2026
- Rumelhart DE, Hinton GE, Williams RJ (1986) Learning representations by back-propagating errors. *Nature* 323:533–536
- Simmons AJ, Willett JK, Jones PD, Thome PW, Dee DP (2010) Low-frequency variations in surface atmospheric humidity, temperature, and precipitation: inferences from reanalyses and monthly gridded observational data sets. *J Geophys Res* 115, D01110. doi:10.1029/2009JD012442
- Tanré D, Kaufman YJ, Herman M, Mattoo S (1997) Remote sensing of aerosol properties over oceans using the MODIS/EOS spectral radiances. *J Geophys Res* 102(D14):16971–16988
- Thompson DWJ, Wallace JM, Jones PD, Kennedy JJ (2009) Identifying signatures of natural climate variability in time series of global-mean surface temperature: methodology and insights. *J Clim* 22:6120–6141
- Van Donkelaar A, Martin RV, Park RJ (2006) Estimating ground-level PM<sub>2.5</sub> using aerosol optical depth determined from satellite remote sensing. *Biogeosciences* D21:201
- Wang J, Christopher SA (2003) Inter comparison between satellite-derived aerosol optical thickness and PM<sub>2.5</sub> mass: implications for air quality studies. *Geophys Res Lett* 30(21):2095
- Wang J, Martin ST (2007) Satellite characterization of urban aerosols: importance of including hygroscopicity and mixing state in the retrieval algorithms. *J Geophys Res* D17203:112
- Yao L, Lu N, Jiang S (2012a) Artificial neural network(ANN) for multi-source PM<sub>2.5</sub> estimation using surface, MODIS, and meteorological data. In: 2012 International Conference on Biomedical Engineering and Biotechnology 1228–1231
- Yao L, Lu N, Shi HD (2012b) Study on spatial-temporal variations in total NO<sub>2</sub> column amounts over China using SCIAMACHY data. *Res Environ Sci* 25(4):419–424 (in Chinese)
- Zhang QH, Zhang JP, Xue HW (2010) The challenge of improving visibility in Beijing. *Atmos Chem Phys* 10:7821–7827